



Published in final edited form as:

Arch Biochem Biophys. 2019 August 15; 671: 8–17. doi:10.1016/j.abb.2019.05.025.

## Hypoxia differentially regulates estrogen receptor alpha in 2D and 3D culture formats

Nathan A. Whitman<sup>1</sup>, Zhi-Wei Lin<sup>1</sup>, Rachael M. Kenney<sup>1</sup>, Leonardo Albertini<sup>1</sup>, Matthew R. Lockett<sup>1,2,\*</sup>

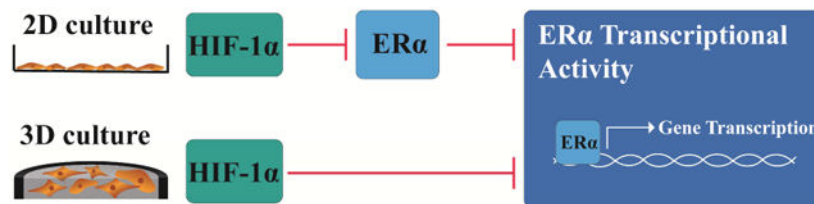
<sup>1</sup>Department of Chemistry, University of North Carolina at Chapel Hill, Kenan and Caudill Laboratories, Chapel Hill, North Carolina 27599-3290

<sup>2</sup>Lineberger Comprehensive Cancer Center, University of North Carolina at Chapel Hill, 450 West Drive, Chapel Hill, North Carolina 27599-7295

### Abstract

Hypoxia is a common feature in solid tumors. Clinical samples show a positive correlation between the expression of the hypoxia-inducible factor HIF-1 $\alpha$  and estrogen receptor alpha (ER $\alpha$ ) and a negative correlation between HIF-1 $\alpha$  and hormone sensitivity. Results from monolayer cultures are in contention with clinical observations, showing that ER (+) cell lines no longer express ER $\alpha$  under hypoxic (1% O<sub>2</sub>) conditions. Here, we compared the impact of hypoxia on the ER $\alpha$  signaling pathway for T47D cells in a 2D and 3D culture format. In the 2D format, the cells were cultured as monolayers. In the 3D format, paper-based scaffolds supported cells suspended in a collagen matrix. Using ELISA, western blot, and immunofluorescence measurements, we show that hypoxia differentially regulates ER $\alpha$  protein levels. In the 2D format, the protein levels are significantly decreased in hypoxia. In the 3D format, the protein levels are maintained in hypoxia. Hypoxia reduced ER $\alpha$  transcriptional activation in both culture formats. These results highlight the importance of considering tissue dimensionality for *in vitro* studies. They also show that ER $\alpha$  protein levels in hypoxia are not an accurate indicator of ER $\alpha$  transcriptional activity, and confirm that a positive stain for ER $\alpha$  in a clinical sample may not necessarily indicate hormone sensitivity.

### Graphical Abstract:



\*Corresponding author: mlockett@unc.edu.

## Keywords

estrogen signaling; hypoxia-inducible factor (HIF); breast cancer

---

## 1. Introduction

Breast cancer is the most commonly occurring cancer in women worldwide [1]. Approximately 70% of breast cancers stain positively for estrogen receptor alpha (ER $\alpha$ ) [2] and rely on estrogen to regulate genes required for proliferation, differentiation, and motility [3-5]. Endocrine therapies—including aromatase inhibitors, selective estrogen receptor modulators, and selective estrogen receptor disruptors—are used as adjuvant therapies, preventing breast tumor growth and recurrence by targeting proteins involved in the ER $\alpha$  signaling pathway [6-8].

Nearly 40% of estrogen-sensitive ER (+) tumors become hormone-insensitive [7, 8]. A number of factors have been implicated in this progression, including the tumor microenvironment [6, 8]. Solid tumor masses are often poorly vascularized, resulting in regions of insufficient oxygen tension to support normal cellular functions (hypoxia) [9]. In healthy breast tissue, the average partial pressure of oxygen (pO<sub>2</sub>) is 52.0 mmHg (6.8%). The average pO<sub>2</sub> for 212 breast tumors ranging in size and stage was hypoxic at 10.0 mmHg (1.3%) [10, 11]. Hypoxia is associated with both tumor recurrence and aggressiveness in breast cancer [9, 12].

Hypoxia-inducible factor 1 (HIF-1) is a master regulator of cellular responses in hypoxic conditions [12], regulating the expression of more than 70 target genes involved in angiogenesis, tissue remodeling, metabolism, and proliferation [13-15]. This heterodimeric transcription factor consists of an oxygen-sensitive  $\alpha$  subunit and a stable  $\beta$  subunit. Under normoxic conditions, HIF-1 $\alpha$  is readily targeted for degradation by prolyl-4-hydroxylases (PHDs) and the von Hippel-Lindau tumor suppressor. Under hypoxic conditions, HIF-1 $\alpha$  is stabilized and able to translocate to the nucleus, where it forms an active transcription factor complex.

HIF-1 $\alpha$  protein stabilization has been associated with endocrine therapy insensitivity in ER (+) breast cancer patients and its expression is positively correlated with ER $\alpha$  expression in tissue samples [16-18]. Interestingly, previous *in vitro* studies exposing monolayer cultures of ER (+) breast cell lines to hypoxic conditions (1% O<sub>2</sub>, 24 – 48 h) had significantly reduced ER $\alpha$  protein levels [19, 20]. The discrepancy between clinical and *in vitro* studies led us to question if the 3D tumor environment alters the interplay between the hypoxia and ER $\alpha$  signaling pathways within *in vitro* models.

Three-dimensional (3D) culture models emulate key aspects of the tumor microenvironment [21-24]. Both ER $\alpha$  and HIF-1 $\alpha$  signaling pathways are sensitive to the culture environment. Vantangoli *et al.* showed that transcriptional regulation in the ER (+) MCF-7 cell line was markedly different for monolayers or microtissues in an agarose gel exposed to 17 $\beta$ -estradiol (E2) [25]. After 24 h, five gene transcripts increased above basal levels in the 2D cultures, whereas 22 transcripts were either increased or decreased in the 3D cultures. In

another study, DelNero *et al.* found that 214 genes were differentially regulated when OSCC-3 cells in monolayers or suspended in alginate discs were exposed to hypoxia for six days [26]. In particular, they observed increased expression of pro-inflammatory genes in 3D culture, compared to levels seen in 2D culture.

There is not a study to our knowledge that compares how the transition from 2D to a 3D culture format affects the interplay between the HIF-1 $\alpha$  and ER $\alpha$  signaling pathways. In this work, we compared the impact of 24 h of hypoxia on the expression and transcriptional activity of ER $\alpha$  in 2D and 3D culture formats. The 2D cultures were monolayers on plasticware and the 3D cultures were cell-containing collagen suspensions in wax-patterned paper scaffolds. The paper scaffolds, which allow thin gel slabs (40 microns thick) to be easily manipulated without fear of cracking or breaking, have been used to generate 3D models of breast [27-30], lung [31, 32], colon [33], ovarian and cervical [34], and head and neck tumors [35]. Our studies show that both the HIF-1 $\alpha$  and the ER $\alpha$  signaling pathways of the T47D-KBluc cell line are differentially regulated in different culture formats. In particular, ER $\alpha$  levels in 3D cultures are not impacted by hypoxia, yet ER $\alpha$  transcriptional activity is decreased under hypoxia in both 2D and 3D culture formats.

## 2. Materials and methods

### 2.1 Materials

All reagents were used as received unless otherwise stated. 17 $\beta$ -estradiol (E2) and MG-132 were purchased from Sigma-Aldrich. Dimethylxalylglycine (DMOG) was purchased from Frontier Scientific. Cell culture medium and additives were purchased from Gibco, except for collagen I (rat tail, Corning), DMSO (Fisher Scientific), ethanol (Fisher Scientific), and fetal bovine serum (FBS, VWR). CellTiter-Glo, ONE-Glo, and Reporter Lysis 5X Buffer were purchased from Promega and used according to the manufacturer's protocols.

### 2.2 Cell culture

The T47D-KBluc (T47D) cell line was kindly provided by Dr. Vickie Wilson at the EPA. These cells are an engineered variant of the ER (+) T47D cell line that expresses luciferase, in a dose-dependent manner, in the presence of estrogenic agonists [36]. The cells were cultured as monolayers in phenol red-free DMEM supplemented with 10% FBS, 4.5 g/L D-glucose, 4 mM L-glutamine, 25 mM HEPES, 1 mM sodium pyruvate, 0.1 mM nonessential amino acids, 0.5 mg/mL Geneticin, and 0.05 mg/mL gentamicin. Cells were maintained at 37 °C in a 5% CO<sub>2</sub> environment. Culture medium was exchanged every 2-3 days, and the cells were passed at a 1:10 dilution upon confluency. Unless otherwise stated, the cells were placed in withdrawal medium 3 d prior to use. Withdrawal medium consisted of phenol red-free DMEM supplemented with 10% charcoal-stripped FBS, 4.5 g/L D-glucose, 4 mM L-glutamine, 25 mM HEPES, 1 mM sodium pyruvate, 0.1 mM nonessential amino acids, and 0.05 mg/mL gentamicin.

For 2D cultures, the T47D cells were seeded at a density of 40,000 cells/well in tissue culture-treated 96-well plates. For 3D cultures, the T47D cells were suspended in 1.2 mg/mL collagen I at a density of 40,000 cells/ $\mu$ L. Paper scaffolds containing a single zone

surrounded by a wax-patterned border were seeded with 1  $\mu\text{L}$  of the cell-containing suspension, a final density of  $4 \times 10^7$  cells/cm<sup>3</sup>. The paper scaffolds are detailed in Fig. S1. Their preparation and characterization have been previously detailed [27].

For normoxia studies, cells were maintained at 21% oxygen in a standard cell culture incubator. For hypoxia studies, cells were maintained at 1% oxygen in an O<sub>2</sub> Control In Vitro Glove Box (Coy Laboratory Products). Both culture environments maintained the cells at 37 °C in a 5% CO<sub>2</sub> environment.

### 2.3 ELISA and western blot

Prior to ELISA and western blot analysis, cells in both the 2D and 3D cell culture formats were lysed in ice-cold RIPA buffer (20 min, frequent agitation, 4 °C,  $2 \times 10^6$  cells per mL of lysis buffer). The resulting lysates were clarified by centrifugation at 10,000  $\times g$  at 4 °C for 10 min. For ELISA, ER $\alpha$  and HIF-1 $\alpha$  concentrations were determined with commercial kits (R&D Systems, DYC-5715 and DYC1935);  $\beta$ -actin concentration was determined with a sandwich assay consisting of a  $\beta$ -actin capture antibody (R&D Systems, AF4000) and an HRP-linked detection antibody (SantaCruz Biotechnology, sc-47778).

For western blot analyses, clarified lysates were separated by SDS-PAGE and transferred to PVDF membranes. Membranes were probed with antibodies for ER $\alpha$  (1:500), HIF-1 $\alpha$  (1:200), and  $\beta$ -actin (1: 500), detected with HRP-conjugated secondary antibodies (1: 1000 m-IgG<sup>o</sup> BP-HRP), and visualized with the Pierce ECL Plus Western blotting substrate. Antibodies for ER $\alpha$  (sc-8002),  $\beta$ -actin (sc-47778), and mIgG<sup>o</sup> BP-HRP (sc-516102) were purchased from Santa Cruz Biotechnology; the HIF-1 $\alpha$  antibody (610958) was purchased from BD Transduction Laboratories.

### 2.4 Immunofluorescence staining

Withdrawn cells were seeded on glass coverslips or in paper scaffolds. The cells were incubated for 24 h under normoxic or hypoxic conditions, in the presence of either vehicle (0.1% ethanol) or 10 nM E2. The coverslips and paper scaffolds were washed with 1X PBS, fixed with 3.2% paraformaldehyde in 1X PBS for 15 min, blocked for 1 hr in 1X PBS containing 5% normal goat serum and 0.3% Triton X-100, and incubated overnight in anti-ER $\alpha$  (1:100, Santa Cruz Biotechnology sc-8002). The stained samples were washed with 1X PBS containing 0.3% Triton X-100, and incubated with IgG-CFL 555 (1:200, goat anti-mouse, Santa Cruz Biotechnology sc-362267) and DAPI (1:1000) for 3 h. Stained samples were washed with 1X PBS containing 0.3% Triton X-100 and with 1X PBS before mounting on glass microscope slides with ProLong Gold Antifade Mountant (Invitrogen). Mounted samples were sealed with clear nail polish and allowed to cure overnight before image acquisition.

### 2.5 Fluorescence image acquisition and analysis

Fluorescence micrographs were obtained on a Zeiss LSM 710 confocal laser scanning microscope using a 25x/0.8 LD LCI Plan-Apochromatic objective. For 2D cultures, a single confocal image was acquired; for 3D cultures, z-stack images were taken every 5  $\mu\text{m}$ . Each image (512  $\times$  512 pixels) is the average of six scans obtained at an acquisition speed of 1.27

$\mu\text{s}/\text{pixel}$ , using a 36  $\mu\text{m}$  pinhole. ER $\alpha$  was imaged with a 543/604 nm filter set and DAPI with a 405/478 filter set.

Single-slice images from each z-stack were analyzed with FIJI using the following procedure. First, the DAPI images were automatically thresholded using the Otsu method [37]. Next, we generated a binary mask for each nucleus. Regions of interest (ROIs) were then generated from each nuclear mask using the analyze particles function (parameters: size = 20 – 250  $\mu\text{m}$  and circularity = 0.2 – 1.0). These ROIs were applied to the ER $\alpha$  images to measure the intensity of nuclear ER $\alpha$  staining. The raw intensity data for each culture format was normalized to the intensity signal for cultures incubated under normoxia in E2-deprived medium.

## 2.6 RNA isolation and RT-qPCR

Total RNA was isolated from both 2D and 3D cultures after a 24 h treatment using the TRIzol Plus RNA Purification Kit (Thermo Fisher Scientific); 1  $\mu\text{g}$  of RNA was reverse transcribed with the High-Capacity cDNA Reverse Transcription Kit (Thermo Fisher Scientific). Each qPCR reaction (10  $\mu\text{L}$  total volume) was prepared in a 384-well plate with 0.3  $\mu\text{M}$  primers and PowerUp SYBR Green PCR Master Mix (Applied Biosystems). qPCR was performed with a QuantStudio 6 Flex Real-Time PCR System (Applied Biosystems) using the following amplification protocol: initial denaturation at 95.0  $^{\circ}\text{C}$  for 20 seconds followed by 40 cycles of 2 seconds at 95  $^{\circ}\text{C}$  and 30 seconds at 60  $^{\circ}\text{C}$ . The primers for estrogen receptor  $\alpha$  (*ESR1*), progesterone receptor (*PGR*), hypoxia-inducible factor 1 $\alpha$  (*HIF1A*), vascular epidermal growth factor A (*VEGFA*) and  $\beta$ -actin (*ACTB*) are listed in Table S1. Standard curves for each primer pair were generated and the efficiency of each qPCR reaction was calculated (Fig. S2). Relative quantification of target genes was performed in triplicate and analyzed with the  $C_t$  method using  $\beta$ -actin (*ACTB*) as the reference gene [38].

## 2.7 ER transcriptional activation assay

ER $\alpha$  transcriptional activation was measured as described previously [27]. Withdrawn cells were seeded at a density of 40,000 cells per 100  $\mu\text{L}$  in a 96-well plate or seeded in paper scaffolds at 40,000 cells per zone. Luciferase activity and cellular viability were assessed with the One-Glo and CellTiter-Glo reagents, respectively. For each assay, cells were lysed in ambient oxygen conditions for 30 min. All of the luciferase activity reactions were also performed under ambient oxygen levels. Luminescence values were recorded on a SpectraMax M5 plate reader and are reported as a fold-change relative to the cultures incubated in E2-deprived medium under normoxia.

## 2.8 *In vitro* proteasome activity assay

*In vitro* proteasome activity was assessed using a fluorescence-based assay (ab107921, Abcam). Briefly,  $2 \times 10^6$  cells were lysed in 400  $\mu\text{L}$  NP-40 lysis buffer (20 min, frequent agitation, 4  $^{\circ}\text{C}$ ). The lysate was clarified by centrifugation. Activity reactions were prepared by adding 20  $\mu\text{L}$  of sample to 80  $\mu\text{L}$  of assay buffer in either the absence or presence of the proteasome inhibitor MG-132 (100  $\mu\text{M}$ ). The reactions were initiated by the addition of 1  $\mu\text{L}$  of fluorogenic proteasome substrate, incubated at 37  $^{\circ}\text{C}$  for 30 min, and then the

fluorescence intensity recorded for an additional 30 min (Ex350/440). Proteasome activity was normalized to the total protein from each reaction, determined with a BCA assay (Pierce).

## 2.9 Statistics

Unless otherwise specified, each dataset represents the average and standard error of the mean (SEM) of at least six replicates. GraphPad Prism v7.0b was used for statistical analyses. Two groups were compared using an unpaired Student's *t*-test with Welch's correction; multiple comparisons were made using one-way ANOVA. A *p* value of < 0.05 was considered significant.

## 3. Results

### 3.1 ER $\alpha$ levels are insensitive to hypoxia in a 3D culture format

To evaluate the impact of decreased oxygen tension on ER $\alpha$  protein expression, we exposed both monolayers and 3D cultures containing 40,000 T47D cells to either normoxic (~21% O<sub>2</sub>) or hypoxic (1% O<sub>2</sub>) conditions for 24 h. Schematics of both culture formats are shown in Fig. 1A. We quantified ER $\alpha$  levels, after lysis, with an ELISA.

In both culture formats under normoxic conditions, ER $\alpha$  significantly decreased upon exposure to E2, consistent with previous reports using monolayer cultures [39-41]. In 2D, the ER $\alpha$  decrease was greater (1022 to 484 pg/mL, Fig. 1B) than in 3D (1204 to 634 pg/mL, Fig. 1C). Hypoxia significantly reduced ER $\alpha$  expression in 2D cultures in both E2-deprived (3.8-fold decrease) and E2-supplemented (2.9-fold decrease) medium. These findings agree with previous *in vitro* studies [19, 20, 42]. Surprisingly, ER $\alpha$  expression levels were not affected by hypoxia in the 3D cultures. Western blots confirmed the ELISA results, showing that the fold-changes were representative of full-length ER $\alpha$  and not artifacts caused by ER $\alpha$  truncates or degradation products. Fig. 1D is a representative set of western blots; Fig. S3 summarizes relative band intensities from three biological replicates.

To determine if the ELISA results were representative of all cells in the culture, we assessed nuclear localization of ER $\alpha$  with immunofluorescence. Representative single-plane images of cells in both culture formats are displayed in Fig. 2A and 2B. To quantify nuclear localization of ER $\alpha$ , we used DAPI-stained nuclei to generate co-localized regions of interest, as described previously [43]. Fig. 2C and 2D contain frequency distributions of ER $\alpha$  nuclear staining for the 2D and 3D culture formats, respectively. The fluorescence intensity of nuclear ER $\alpha$  staining for each condition was normalized to the average fluorescence intensity of cultures incubated in E2-deprived medium under normoxic conditions. Each frequency distribution could be fit to a single Gaussian (Fig. S4) with R<sup>2</sup> values above 0.9 (Table S2). These results indicate a unimodal response and demonstrate that the average changes in ER $\alpha$  levels are representative of the entire population of cells rather than a subpopulation of strongly expressing cells. The average fluorescence intensity of nuclear ER $\alpha$  staining in 2D (Fig. 2E) and 3D (Fig. 2F) culture formats are an alternative means of displaying this dataset, and further confirm that ER $\alpha$  is sensitive to E2 in both



culture formats and that ER $\alpha$  is sensitive to hypoxia in the 2D culture format but not in the 3D culture format.

### 3.2 Cells in both culture formats undergo classic responses to hypoxia

To confirm that cells in both culture formats underwent a canonical response to hypoxia, we repeated the experimental setups detailed above and quantified HIF-1 $\alpha$  levels with both ELISA (Fig. 3A and 3B) and western blot (Fig. S5). The basal levels of HIF-1 $\alpha$  were the same in both culture formats, suggesting that the cells in the scaffolds were well oxygenated. HIF-1 $\alpha$  levels increased significantly after a 24 h exposure to hypoxia, with a culture format-dependent stabilization: a 9.5-fold increase in 2D and a 3.0-fold increase in 3D.

Previous studies showed that hypoxia does not have an impact on *HIF1A* expression [44], and that increased levels of HIF-1 $\alpha$  are caused by a decrease in its rate of degradation [15]. We quantified the relative abundance of both *HIF1A* and *VEGFA*, a classic HIF-responsive gene, using RT-qPCR. As expected, hypoxia had no impact on relative *HIF1A* abundance in any of the setups (Fig. 3C and 3D). We observed a significant increase in *VEGFA* mRNA expression under hypoxia in both 2D (Fig. 3E) and 3D (Fig. 3F) culture formats, confirming HIF-1 $\alpha$  transcriptional activity.

### 3.3 ER $\alpha$ is both transcriptionally and post-translationally regulated under hypoxia

Despite an agreement that hypoxia decreases ER $\alpha$  protein expression in 2D, its impact on *ESR1* gene expression is contended. Two separate studies found that hypoxia decreased *ESR1* gene expression in MCF-7 and T47D cells [19, 45]. A third study found hypoxia did not affect *ESR1* in a panel of 10 ER (+) cell lines that included MCF-7 and T47D [20]. We observed a significant reduction in *ESR1* in both culture formats (Fig. 4A and 4B). These results highlight that transcriptional and translational regulation of ER $\alpha$  is not directly related in the 3D cultures.

Previous studies using monolayer cultures determined ER $\alpha$  loss under hypoxic conditions was mediated by the ubiquitin-proteasome system (UPS) [46, 47]. To confirm this finding, we treated both culture formats with MG-132 (10  $\mu$ M), a selective proteasome inhibitor, for 8 h. Under normoxia, HIF-1 $\alpha$  levels were significantly increased in both 2D (Fig. 4C) and 3D (Fig. 4D) formats, confirming proteasome inhibition. Under hypoxic conditions, ER $\alpha$  protein levels increased significantly in both 2D (Fig. 4E) and 3D (Fig. 4F) formats, confirming that ER $\alpha$  is, at least partially, regulated by the UPS in hypoxia.

Given the role of the UPS in regulating ER $\alpha$  under hypoxic conditions, we hypothesized that altered proteasome activity could explain the differences in ER $\alpha$  levels between the two culture formats. Liu *et al.* showed that proteasome activity in monolayer cultures of HUVECs and in lung tissue from a mouse model increased after exposure to hypoxia [48]. We measured 26S proteasome activity in cell lysates collected from both culture formats with a fluorescence-based assay. Hypoxia had no impact on proteasomal activity in either culture format, suggesting that the constant levels of ER $\alpha$  in 3D cultures are not caused by altered UPS activity (Fig. S6).

### 3.4 Hypoxia reduces ER $\alpha$ transcriptional activity in both 2D and 3D cultures

To determine if ER $\alpha$  protein levels were an accurate indicator of its transcriptional activity, we quantified luciferase activity in both culture formats with the ONE-Glo assay. Under normoxic and hypoxic conditions, the T47D cells had low basal luciferase activity in both culture formats (Fig. 5A and 5B). Upon treatment with a saturating concentration of E2 (10 nM), luciferase activity increased significantly in each setup. Under normoxic conditions, there was a 68-fold increase in 2D and a 32-fold increase in 3D. Under hypoxic conditions, the increases were muted with an 8-fold increase in 2D and a 7-fold increase in 3D. These results indicate that hypoxia significantly reduced ER $\alpha$  transcriptional activity in both culture formats.

We also quantified the expression of the progesterone receptor (*PGR*), a canonical estrogen receptor target gene. Under normoxic conditions, basal *PGR* levels were similar in both culture formats (Table S3) and increased upon addition of E2 (Fig. 5C and 5D). In both culture formats, hypoxia significantly decreased *PGR* expression in E2-deprived and -supplemented medium, mirroring trends observed using the luciferase transcriptional activation assay.

### 3.5 ER $\alpha$ transcriptional activity is decreased by chemical stabilization of HIF-1 $\alpha$

To determine whether ER $\alpha$  expression levels and transcriptional activity were mediated by HIF-1 $\alpha$  or a different hypoxia-mediated mechanism (e.g., increased mitochondrial reactive oxygen species), we treated cultures with DMOG (1 mM). This small molecule stabilizes HIF-1 $\alpha$  under normoxia by inhibiting PHD activity. ER $\alpha$  and HIF-1 $\alpha$  protein levels in cell lysates were quantified with an ELISA; ER $\alpha$  transcriptional activity was measured with the ONE-Glo assay.

In both culture formats, DMOG stabilized HIF-1 $\alpha$  levels in normoxia (Fig. 6A and 6B), confirming inhibition of PHD. The DMOG had culture-dependent effects, with significant decreases in ER $\alpha$  for 2D cultures in the presence and absence of E2 (Fig. 6C); a small but significant increase in ER $\alpha$  for 3D cultures in the absence of E2 (Fig. 6D); and no change in ER $\alpha$  in E2-treated cultures (Fig. 6D). In both culture formats DMOG decreased ER $\alpha$  transcriptional activation in the presence of E2 (Fig. 6E and 6F).

Together, these results suggest that HIF-1 $\alpha$  is responsible for the significant reduction of ER $\alpha$  transcriptional activity observed under hypoxic conditions in both culture formats. HIF-1 $\alpha$  is also responsible for the loss of ER $\alpha$  protein expression in 2D culture formats. Neither hypoxia nor stabilization of HIF-1 $\alpha$  significantly impacted ER $\alpha$  protein expression in 3D culture formats.

## 4. Discussion

The dysregulated expression of ER $\alpha$  is common in tumors of hormone-sensitive tissues, including breast, ovary, and thyroid [4, 49-51]. Progression of ER (+) breast tumors from hormone-responsive to hormone-insensitive is associated with a poor prognosis, as the cancers no longer respond to adjuvant endocrine therapies [8, 52]. Clinical samples of hormone-insensitive ER (+) tumors co-stain for HIF-1 $\alpha$  and ER $\alpha$ , suggesting that hypoxia



has a role in promoting this transition [16, 17, 53]. Hypoxia also decreases hormone sensitivity in monolayer cultures. This decrease is coupled with decreased ER $\alpha$  protein levels, suggesting that activity is directly related to protein availability. In our experimental setup, we determined that culture format significantly altered ER $\alpha$  regulation in the T47D cell line, when exposed to hypoxic conditions.

In both formats, the cells underwent a canonical HIF-1 $\alpha$  stabilization upon exposure to hypoxic conditions [9, 30, 54, 55]. The extent of this stabilization was four-fold greater in the 2D format, but was not reflected in overall transcriptional activity as both culture formats had a nearly six-fold increase in *VEGF* expression. We are unaware of a single study that directly compared HIF-1 $\alpha$  stabilization between 2D and 3D culture formats, but discrepancies in transcriptional activity have been noted previously [26]. Cells in both formats had similar levels of HIF-1 $\alpha$  under normoxic conditions, suggesting the cells in the 40- $\mu$ m thick scaffolds were not hypoxic. Our previous characterization of a paper-based colon tumor model showed that scaffolds containing similar cell densities had oxygen tensions of less than 21% but were still within the clinically accepted values of normoxia [10, 33]. These results are also supported by previous work, which showed that hypoxia occurs in a tissue, multicellular aggregate, or collagen I suspension when the distance between the cells and the oxygen source exceeds 150  $\mu$ m [10, 56, 57]. Based on previous comparisons of oxygen and glucose gradients in spheroids, we can also conclude that the cells in the paper scaffolds were not experiencing nutrient starvation [58].

In normoxia, the basal ER $\alpha$  levels and transcriptional activity were similar in both culture formats. The changes in ER $\alpha$  levels caused by hypoxia were, however, markedly different when moving from a 2D to a 3D culture format. Hypoxia decreased *ESR1* levels in both culture formats, which is supported by previous studies in monolayers [19, 45], and suggests ER $\alpha$  is regulated at either the translational or post-translational level.

When exposed to hypoxic conditions, ER $\alpha$  levels were significantly reduced in the 2D format. A similar reduction also occurred in the presence of E2. These results agree with previous *in vitro* experiments [19, 20, 42]. The combination of hypoxia and E2 decreased ER $\alpha$  in monolayer cultures, but did not have an obvious additive or cooperative response. The use of a PHD inhibitor, which stabilized HIF-1 $\alpha$  under normoxia, confirmed a HIF-1 $\alpha$ -dependent process caused these changes in ER $\alpha$ . While E2 decreased ER $\alpha$  in the 3D cultures, neither hypoxia nor the stabilization of HIF-1 $\alpha$  altered its expression.

While there are no direct comparisons of ER $\alpha$  expression between 2D and 3D cultures, others have evaluated ER $\alpha$  in spheroids. Truchet *et al.* found uniform levels of ER $\alpha$  across MCF-7 spheroids (~ 400  $\mu$ m in diameter) that possessed proliferative gradients [59]. The addition of E2 decreased these levels across the spheroid, with no differences between the oxygen-rich periphery and the oxygen-poor core. These results support our observations that hypoxia had no impact on ER $\alpha$  expression in 3D culture. Counter to our findings, Munoz *et al.* showed that larger MCF-7 spheroids (~ 800  $\mu$ m in diameter) lost ER $\alpha$  expression in all but a few cells along the periphery [60]. These studies, however, make it difficult to isolate the impacts of hypoxia on ER $\alpha$  expression from the multiple gradients known to form across spheroids of greater than 150 - 200 microns [57].

The observed decreases in ER $\alpha$  upon addition of E2 was expected because its transcriptional activation enables the subsequent proteolysis by the 26S proteasome [41]. Our proteasome inhibition studies confirmed that ER $\alpha$  was degraded by the UPS under normoxic and hypoxic conditions. Proteasomal activity was similar in both culture formats and unaffected by hypoxia, suggesting that the increased stability of ER $\alpha$  in the 3D culture environment is a result of differential post-translational regulation.

The insensitivity of ER $\alpha$  protein levels to hypoxia in the 3D culture format raises questions about the environmentally mediated regulation of the receptor at either the transcriptional or post-translational level. This increased stability of ER $\alpha$  in the 3D culture formats may be a result of transcriptional repression of E3 ubiquitin ligases [61-64]; increased levels of proteins that directly interact with ER $\alpha$  and increase its stability [65-69]; or altered kinase activities, which can alter the affinity of ER $\alpha$  to other proteins through an altered phosphorylation status [65, 66]. Numerous studies have observed altered kinase activities between 2D and 3D culture formats [23, 70]. It is also possible that the availability of shared E3 ubiquitin ligases or stabilizing proteins is different between 2D and 3D cultures, impacting the stability of ER $\alpha$  under hypoxic conditions [71].

Despite differential regulation of ER $\alpha$  protein levels in the 2D and 3D cultures, hypoxia decreased its transcriptional activity in both culture formats. We attribute the decreased luciferase activity in hypoxia to reduced transcriptional activity of ER $\alpha$  specifically and not to changes in overall translation efficiency. Previous reports support this assumption and show that translation efficiency in breast cancer cell lines is unaffected by moderate hypoxia [20, 72]. Using a selective inhibitor of PHD, we showed that this decrease is mediated by HIF-1 $\alpha$ . One possibility for this decrease in activity is the competition for shared transcriptional coactivators (e.g., p300/CPB and SRC3) [73-75]. Alternatively, decreases in the amount of ER $\alpha$  relative to ER $\beta$  could result in a decrease in ER $\alpha$  transcriptional activity independent of absolute ER $\alpha$  protein levels [19, 76].

In summary, we highlight the importance of incorporating a tissue-like microenvironment when predicting cellular responses to hypoxia. By simply placing cells in a collagen matrix, we found a differential regulation of ER $\alpha$  expression levels. Hypoxia decreased the transcriptional activity of ER $\alpha$  in both culture formats. The significant decrease in ER $\alpha$  in 2D cultures suggested that loss of activity required loss of protein. The stabilization of ER $\alpha$  in 3D cultures, however, can explain both co-staining for HIF-1 $\alpha$  and ER $\alpha$  and hormone insensitivity in clinical samples. Future studies on the hypoxia-mediated progression of breast cancer using a 3D culture platform will likely reveal novel insights into the role of hypoxia in regulating ER $\alpha$  protein levels and transcriptional activity, along with *de novo* and acquired resistance to endocrine therapies used for treatment.

## Supplementary Material

Refer to Web version on PubMed Central for supplementary material.

## Acknowledgments

This work was supported by funds provided by the National Center for Advancing Translational Science (NCATS) through Grant Award Number UL1TR001111 and the National Institute of General Medical Science through Grant Award Number R35GM128697. NAW and RMK thank the Graduate School at UNC for support through Dissertation Completion Fellowships. ZWL and LA thank the NC Louis Stokes Alliance for Minority Participation, NSF Grant Number 1202467, for summer research support. We thank Professor Qing Zhang for access to his hypoxic culture chamber and Melanie Sinanian for helpful feedback and discussion.

## Abbreviations:

|                                 |                                   |
|---------------------------------|-----------------------------------|
| <b>2D</b>                       | two dimensional                   |
| <b>3D</b>                       | three dimensional                 |
| <b>ER<math>\alpha</math></b>    | estrogen receptor alpha           |
| <b>ER (+)</b>                   | estrogen receptor positive        |
| <b>ELISA</b>                    | enzyme-linked immunosorbent assay |
| <b>HIF-1<math>\alpha</math></b> | hypoxia inducible factor 1 alpha  |

## References

- [1]. Cancer Facts & Figures, in: A.C. Society (Ed.) American Cancer Society, Atlanta, 2019.
- [2]. Castoria G, Migliaccio A, Giovannelli P, Auricchio F, Cell proliferation regulated by estradiol receptor: Therapeutic implications, *Steroids* 75(8-9) (2010) 524–527. [PubMed: 19879889]
- [3]. Heldring N, Pike A, Andersson S, Matthews J, Cheng G, Hartman J, Tujague M, Strom A, Treuter E, Warner M, Gustafsson JA, Estrogen receptors: How do they signal and what are their targets, *Physiol. Rev* 87(3) (2007) 905–931. [PubMed: 17615392]
- [4]. Deroo BJ, Korach KS, Estrogen receptors and human disease, *J. Clin. Invest* 116(3) (2006) 561–570. [PubMed: 16511588]
- [5]. Bouris P, Skandalis SS, Piperigkou Z, Afratis N, Karamanou K, Aletras AJ, Moustakas A, Theocharis AD, Karamanos NK, Estrogen receptor alpha mediates epithelial to mesenchymal transition, expression of specific matrix effectors and functional properties of breast cancer cells, *Matrix Biol.* 43(1) (2015) 42–60. [PubMed: 25728938]
- [6]. De Marchi T, Foekens JA, Umar A, Martens JWM, Endocrine therapy resistance in estrogen receptor (ER)-positive breast cancer, *Drug Discov. Today* 21(7) (2016) 1181–1188. [PubMed: 27233379]
- [7]. Osborne CK, Schiff R, Mechanisms of endocrine resistance in breast cancer, *Annu. Rev. Med* 62(1) (2011) 233–247. [PubMed: 20887199]
- [8]. Musgrove EA, Sutherland RL, Biological determinants of endocrine resistance in breast cancer, *Nat. Rev. Cancer* 9(9) (2009) 631–643. [PubMed: 19701242]
- [9]. Semenza GL, The hypoxic tumor microenvironment: A driving force for breast cancer progression, *Biochim. Biophys. Acta, Mol. Cell Res* 1863(3) (2016) 382–391.
- [10]. McKeown SR, Defining normoxia, physoxia and hypoxia in tumours: Implications for treatment respon, *Br. J. Radiol* 87(1035) (2014) 20130676. [PubMed: 24588669]
- [11]. Vaupel P, Hockel M, Mayer A, Detection and characterization of tumor hypoxia using pO<sub>2</sub> histography, *Antioxid. Redox. Signal* 9(8) (2007) 1221–1235. [PubMed: 17536958]
- [12]. Gilkes DM, Semenza GL, Role of hypoxia-inducible factors in breast cancer metastasis, *Future Oncol.* 9(11) (2013) 1623–1636. [PubMed: 24156323]
- [13]. Hickey MM, Simon MC, Regulation of angiogenesis by hypoxia and hypoxia-inducible factors, *Curr. Top. Dev. Biol* 76(1) (2006) 217–257. [PubMed: 17118268]

- [14]. Chiche J, Brahimi-Horn MC, Pouyssegur J, Tumor hypoxia induces a metabolic shift causing acidosis: A common feature in cancer, *J. Cell. Mol. Med* 14(4) (2010) 771–794. [PubMed: 20015196]
- [15]. Semenza GL, HIF-1 and mechanisms of hypoxia sensing, *Curr. Opin. Cell Biol* 13(2) (2001) 167–171. [PubMed: 11248550]
- [16]. Generali D, Berruti A, Brizzi MP, Camp L, Bonardi S, Wigfield S, Bersiga A, Allevi G, Milani M, Aguggini S, Gandolfi V, Dogliotti L, Bottini A, Harris AL, Fox SB, Hypoxia-inducible factor-1 alpha-expression predicts a poor response to primary chemoendocrine therapy and disease-free survival in primary human breast cancer, *Clin. Cancer Res* 12(15) (2006) 4562–4568. [PubMed: 16899602]
- [17]. Bos R, van der Groep P, Greijer AE, Shvarts A, Meijer S, Pinedo HM, Semenza GL, van Diest PJ, van der Wall E, Levels of hypoxia-inducible factor-1 alpha independently predict prognosis in patients with lymph node negative breast carcinoma, *Cancer* 97(6) (2003) 1573–1581. [PubMed: 12627523]
- [18]. Bos R, Zhong H, Hanrahan CF, Mommers ECM, Semenza GL, Pinedo HM, Abeloff MD, Simons JW, van Deist PJ, van der Wall E, Levels of hypoxia-inducible factor-1a during breast carcinogenesis, *JNCI, J. Natl. Cancer Inst* 93(4) (2001) 309–314. [PubMed: 11181778]
- [19]. Wolff M, Kosyna FK, Dunst J, Jelkmann W, Depping R, Impact of hypoxia inducible factors on estrogen receptor expression in breast cancer cells, *Arch. Biochem. Biophys* 613 (2017) 23–30. [PubMed: 27823907]
- [20]. Padro M, Louie RJ, Lananna BV, Krieg AJ, Timmerman LA, Chan DA, Genome-independent hypoxia repression of estrogen receptor alpha in breast cancer cells, *BMC Cancer* 17 (2017) 203. [PubMed: 28320353]
- [21]. Yamada KM, Cukierman E, Modeling tissue morphologies and cancer in 3D, *Cell* 130(4) (2007) 601–610. [PubMed: 17719539]
- [22]. Vantangoli MM, Madnick SJ, Huse SM, Weston P, Boekelheide K, MCF-7 human breast cancer cells form differentiated microtissues in scaffold-free hydrogels, *PLoS Med.* 10(8) (2015) e0135426.
- [23]. Breslin S, O'Driscoll L, The relevance of using 3D cell cultures, in addition to 2D monolayer cultures, when evaluating breast cancer drug sensitivity and resistance, *Oncotarget* 7(29) (2016) 45745–45756. [PubMed: 27304190]
- [24]. Barcellos-Hoff MH, Aggeler J, Ram TG, Bissell MJ, Functional differentiation and alveolar morphogenesis of primary mammary cultures on reconstituted basement membrane, *Development* 105(2) (1989) 223–235. [PubMed: 2806122]
- [25]. Vantangoli MM, Madnick SJ, Wilson S, Boekelheide K, Estradiol exposure differentially alters monolayer versus microtissue MCF-7 human breast carcinoma cultures, *PLoS One* 11(7) (2016) e0157997. [PubMed: 27379522]
- [26]. DelNero P, Lane M, Verbridge SS, Kwee B, Kermani P, Hempstead B, Stroock A, Fischbach C, 3D culture broadly regulates tumor cell hypoxia response and angiogenesis via pro-inflammatory pathways, *Biomaterials* 55(1) (2015) 110–118. [PubMed: 25934456]
- [27]. Whitman NA, Lin ZW, DiProspero TJ, McIntosh JC, Lockett MR, Screening estrogen receptor modulators in a paper-based breast cancer model, *Anal. Chem* 90(20) (2018) 11981–11988. [PubMed: 30226366]
- [28]. Kenney RM, Boyce MW, Truong AS, Bagnell CR, Lockett MR, Real-time imaging of cancer cell chemotaxis in paper-based scaffolds, *Analyst* 141(2) (2016) 661–8. [PubMed: 26548584]
- [29]. Kenney RM, Boyce MW, Whitman NA, Kromhout BP, Lockett MR, A pH-sensing optode for mapping spatiotemporal gradients in 3D paper-based cell cultures, *Anal. Chem* 90(3) (2018) 2376–2383. [PubMed: 29323486]
- [30]. Truong AS, Lockett MR, Oxygen as a chemoattractant: confirming cellular hypoxia in paper-based invasion assays, *Analyst* 141(12) (2016) 3874–3882. [PubMed: 27138213]
- [31]. Camci-Unal G, Newsome D, Eustace BK, Whitesides GM, Fibroblasts enhance migration of human lung cancer cells in paper-based coculture system, *Adv. Healthcare Mater* 5(6) (2016) 641–647.

- [32]. Simon KA, Mosadegh B, Minn KT, Lockett MR, Mohammady MR, Boucher DM, Hall AB, Hillier SM, Udagawa T, Eustace BK, Whitesides GM, Metabolic response of lung cancer cells to radiation in a paper-based 3D cell culture system, *Biomaterials* 95(1) (2016) 47–59. [PubMed: 27116031]
- [33]. Boyce MW, LaBonia GJ, Hummon AB, Lockett MR, Assessing chemotherapeutic effectiveness using a paper-based tumor model, *Analyst* 142(15) (2017) 2819–2827. [PubMed: 28702529]
- [34]. Rodenhizer D, Gaude E, Cojocari D, Mahadevan R, Frezza C, Wouters BG, McGuigan AP, A three-dimensional engineered tumour for spatial snapshot analysis of cell metabolism and phenotype in hypoxic gradients, *Nat. Mater* 15(2) (2016) 227–236. [PubMed: 26595121]
- [35]. Young MK, Rodenhizer D, Dean T, D'Arcangelo E, Xu B, Ailles L, McGuigan AP, A TRACER 3D co-culture tumour model for head and neck cancer, *Biomaterials* 164(1) (2018) 54–69. [PubMed: 29490260]
- [36]. Wilson VS, Bobseine K, Gray LE, Development and characterization of a cell line that stably expresses an estrogen-responsive luciferase reporter for the detection of estrogen receptor agonist and antagonists, *Toxicol. Sci* 81(1) (2004) 69–77. [PubMed: 15166400]
- [37]. Otsu N, Threshold selection method from gray-level histograms, *IEEE Trans. Syst. Man. Cybern* 9(1) (1979) 62–66.
- [38]. Livak KJ, Schmittgen TD, Analysis of relative gene expression data using real-time quantitative PCR and the 2(T)(-Delta Delta C) method, *Methods* 25(4) (2001) 402–408. [PubMed: 11846609]
- [39]. Alarid ET, Bakopoulos N, Proteasome-mediated proteolysis of estrogen receptor: A novel component in autologous down-regulation, *Mol. Endocrinol* 13(9) (1999) 1522–1534. [PubMed: 10478843]
- [40]. Eckert RL, Mullick A, Rorke EA, Katzenellenbogen BS, Estrogen-receptor synthesis and turnover in MCF-7 breast-cancer cells measured by a density shift technique, *Endocrinology* 114(2) (1984) 629–637. [PubMed: 6690295]
- [41]. Valley CC, Solodin NM, Powers GL, Ellison SJ, Alarid ET, Temporal variation in estrogen receptor-alpha protein turnover in the presence of estrogen, *J. Mol. Endocrinol* 40(1-2) (2008) 23–34. [PubMed: 18096994]
- [42]. Cho JY, Kim D, Lee SK, Lee YJ, Cobalt chloride-induced estrogen receptor alpha down-regulation involves hypoxia-inducible factor-1 alpha in MCF-7 human breast cancer cells, *Mol. Endocrinol* 19(5) (2005) 1191–1199. [PubMed: 15695373]
- [43]. Lang JD, Berry SM, Powers GL, Beebe DJ, Alarid ET, Hormonally responsive breast cancer cells in a microfluidic co-culture model as a sensor of microenvironmental activity, *Integ. Biol* 5(5) (2013) 807–816.
- [44]. Doe MR, Ascano JM, Kaur M, Cole MD, Myc posttranscriptionally induces HIF1 protein and target gene expression in normal and cancer cells, *Cancer Res.* 72(4) (2012) 949–957. [PubMed: 22186139]
- [45]. Ryu K, Park C, Lee Y, Hypoxia-inducible factor 1 alpha represses the transcription of the estrogen receptor alpha gene in human breast cancer cells, *Biochem. Biophys. Res. Commun* 407(4) (2011) 831–836. [PubMed: 21458421]
- [46]. Stoner M, Saville B, Wormke M, Dean D, Burghardt R, Safe S, Hypoxia induces proteasome-dependent degradation of estrogen receptor alpha in ZR-75 breast cancer cells, *Mol. Endocrinol* 16(10) (2002) 2231–2242. [PubMed: 12351689]
- [47]. Cooper C, Liu GY, Niu YL, Santos S, Murphy LC, Watson PH, Intermittent hypoxia induces proteasome-dependent down-regulation of estrogen receptor in human breast carcinoma, *Clin. Cancer Res* 10(24) (2004) 8720–8727. [PubMed: 15623657]
- [48]. Liu H, Wang Z, Yu S, Xu J, Proteasomal degradation of O-GlcNAc transferase elevates hypoxia-induced vascular endothelial inflammatory response, *Cardiovasc. Res* 103(1) (2014) 131–139. [PubMed: 24788415]
- [49]. Di Vito M, De Santis E, Perrone GA, Mari E, Giordano MC, De Antoni E, Coppola L, Fadda G, Tafani M, Carpi A, Russo MA, Overexpression of estrogen receptor-alpha in human papillary thyroid carcinomas studied by laser-capture microdissection and molecular biology, *Cancer Sci.* 102(10) (2011) 1921–1927. [PubMed: 21707866]

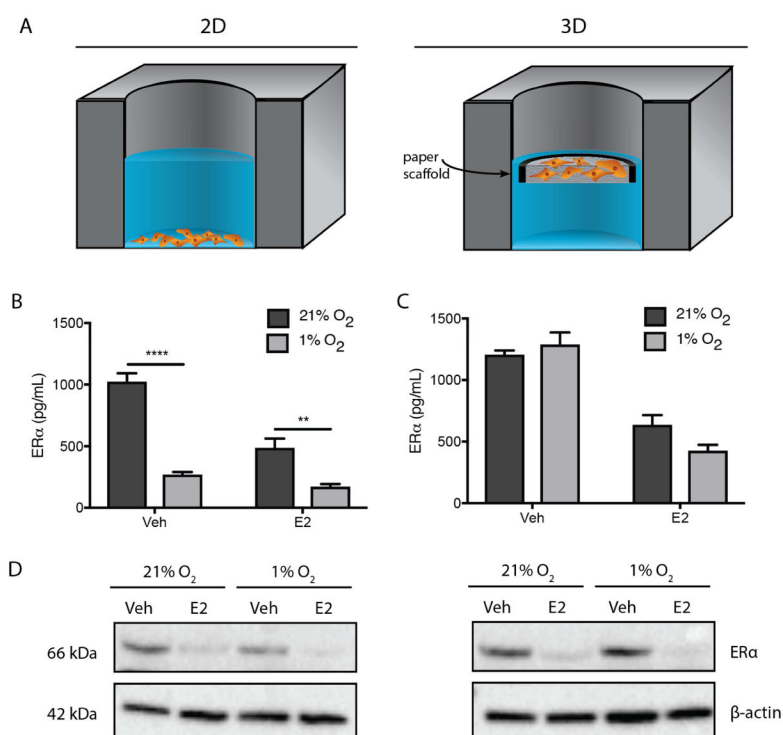
- [50]. Tafani M, Russo A, Di Vito M, Sale P, Pellegrini L, Schito L, Gentileschi S, Bracaglia R, Marandino F, Garaci E, Up-regulation of pro-inflammatory genes as adaptation to hypoxia in MCF-7 cells in human mammary invasive carcinoma microenvironment, *Cancer Sci.* 101(4) (2010) 1014–1023. [PubMed: 20151982]
- [51]. Chan KKL, Siu MKY, Jiang YX, Wang JJ, Wang Y, Leung THY, Liu SS, Cheung ANY, Ngan HYS, Differential expression of estrogen receptor subtypes and variants in ovarian cancer: Effects on cell invasion, proliferation, and prognosis, *BMC Cancer* 17(1) (2017) 606. [PubMed: 28859612]
- [52]. Lopez-Tarruella S, Schiff R, The dynamics of estrogen receptor status in breast cancer: Reshaping the paradigm, *Clin. Cancer Res* 13(23) (2007) 6921–6925. [PubMed: 18056165]
- [53]. Generali D, Buffa FM, Berruti A, Brizzi MP, Campo L, Bonardi S, Bersiga A, Allevi G, Milani M, Aguggini S, Papotti M, Dogliotti L, Bottini A, Harris AL, Fox SB, Phosphorylated ER $\alpha$ , HIF-1 $\alpha$ , and MAPK signaling as predictors of primary endocrine treatment response and resistance in patients with breast cancer, *J. Clin. Oncol* 27(2) (2009) 227–234. [PubMed: 19064988]
- [54]. Lehmann S, Te Boekhorst V, Odenthal J, Bianchi R, van Helvert S, Ikenberg K, Ilina O, Stoma S, Xandry J, Jiang L, Grenman R, Rudin M, Friedl P, Hypoxia induces a HIF-1-dependent transition from collective-to-amoeboid dissemination in epithelial cancer cells, *Curr. Biol* 27(3) (2017) 392–400. [PubMed: 28089517]
- [55]. Daster S, Amatruder N, Calabrese D, Ivanek R, Turrini E, Droesser RA, Zajac P, Fimognari C, Spagnoli GC, Jezzi G, Mele V, Muraro MG, Induction of hypoxia and necrosis in multicellular tumor spheroids is associated with resistance to chemotherapy treatment, *Oncotarget* 8(1) (2017) 1725–1736. [PubMed: 27965457]
- [56]. Szot CS, Buchanan CF, Freeman JW, Rylander MN, 3D in vitro bioengineered tumors based on collagen I hydrogels, *Biomaterials* 32(31) (2011) 7905–7912. [PubMed: 21782234]
- [57]. Hirschhaeuser F, Menne H, Dittfeld C, West J, Mueller-Klieser W, Kunz-Schughart LA, Multicellular tumor spheroids: An underestimated tool is catching up again, *J. Biotechnol* 148(1) (2010) 3–15. [PubMed: 20097238]
- [58]. Milotti E, C. R., Emergent properties of tumor microenvironment in a real-life model of multicell tumor spheroids, *PLoS One* 5(11) (2010) e13942. [PubMed: 21152429]
- [59]. Truchet I, Jozan S, Baron S, Frongia C, Balaguer P, Richard-Foy H, Valette A, Estrogen and antiestrogen-dependent regulation of breast cancer cell proliferation in multicellular spheroids: Influence of cell microenvironment, *Int. J. Oncol* 32(5) (2008) 1033–1039. [PubMed: 18425329]
- [60]. Munoz L, Espinosa M, Quintanar-Jurado V, Hildago A, Melendez-Zajgla J, Maldonado V, Paradoxical changes in the expression of estrogen receptor  $\alpha$  in breast cancer multicellular spheroids, *Tissue Cell* 42(5) (2010) 344–347.
- [61]. Bhatt S, Xiao Z, Meng Z, Katzenellenbogen BS, Phosphorylation by p38 mitogen-activated protein kinase promotes estrogen receptor  $\alpha$  turnover and functional activity via the SCF(Skp2) proteasomal complex, *Mol. Cell Biol* 32(10) (2012) 1928–1943. [PubMed: 22431515]
- [62]. Eakin CM, Maccoss MJ, Finney GL, Klevit RE, Estrogen receptor  $\alpha$  is a putative substrate for the BRCA1 ubiquitin ligase, *Proc. Natl. Acad. Sci. USA* 104(14) (2007) 5794–5799. [PubMed: 17392432]
- [63]. Fan M, Park A, Nephew KP, CHIP (carboxyl terminus of Hsc70-interacting protein) promotes basal and geldanamycin-induced degradation of estrogen receptor- $\alpha$ , *Mol. Endocrinol* 19(12) (2005) 2901–2914. [PubMed: 16037132]
- [64]. Sun J, Zhou W, Kaliappan K, Nawaz Z, Slingerland JM, ER $\alpha$  phosphorylation at Y537 by Src triggers E6-AP-ER $\alpha$  binding, ER $\alpha$  ubiquitylation, promoter occupancy, and target gene expression, *Mol. Endocrinol* 26(9) (2012) 1567–1577. [PubMed: 22865929]
- [65]. Wei X, Xu H, Kufe D, MUC1 oncoprotein stabilizes and activates estrogen receptor  $\alpha$ , *Mol. Cell* 21(2) (2006) 295–305. [PubMed: 16427018]
- [66]. Rajbhandari P, Schalper KA, Solodin NM, Ellison-Zelski SJ, Ping Lu K, Rimm DL, Alarid ET, Pin1 modulates ER $\alpha$  levels in breast cancer through inhibition of phosphorylation-dependent ubiquitination and degradation, *Oncogene* 33(11) (2014) 1438–1447. [PubMed: 23542176]



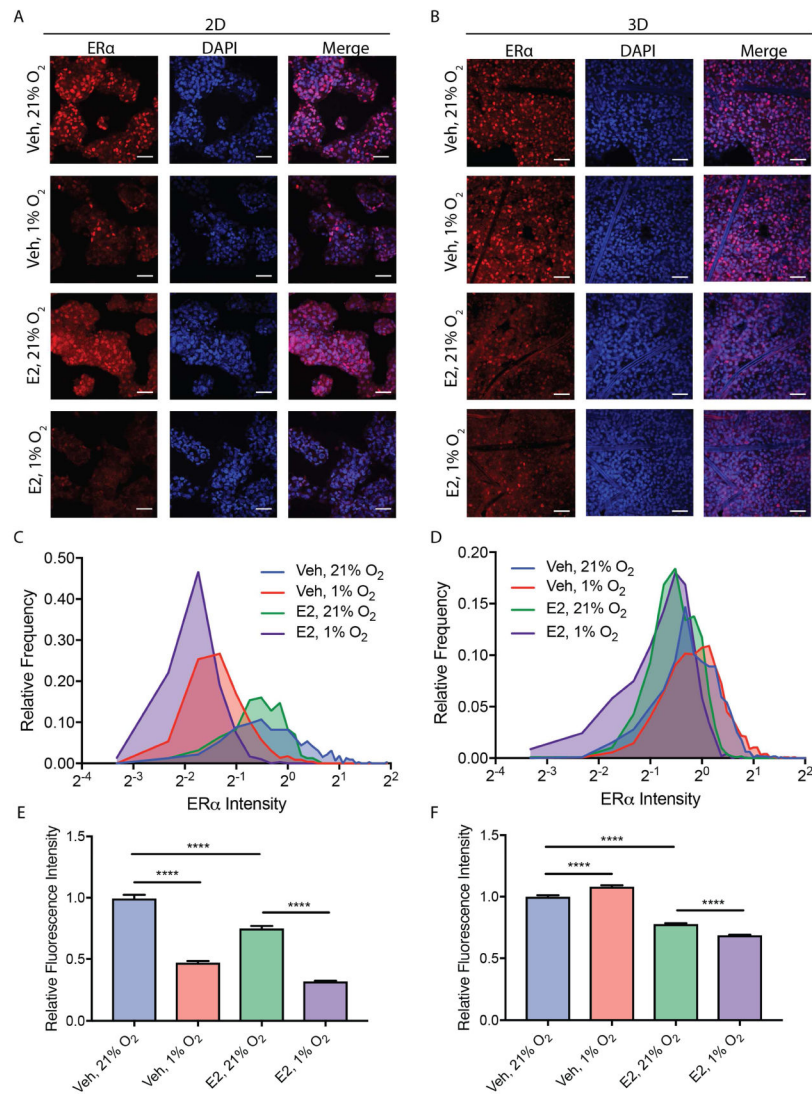
- [67]. Grisouard J, Medunjanin S, Hermani A, Shukla A, Mayer D, Glycogen synthase kinase-3 protects estrogen receptor alpha from proteasomal degradation and is required for full transcriptional activity of the receptor, *Mol. Endocrinol* 21(10) (2007) 2427–2439. [PubMed: 17609434]
- [68]. Giamas G, Filipovic A, Jacob J, Messier W, Zhang H, Yang D, Zhang W, Shifa BA, Photiou A, Tralau-Stewart C, Castellano L, Green AR, Coombes RC, Ellis IO, Ali S, Lenz HJ, Stebbing J, Kinome screening for regulators of the estrogen receptor identifies LMTK3 as a new therapeutic target in breast cancer, *Nat. Med* 17(6) (2011) 715–719. [PubMed: 21602804]
- [69]. He X, Zheng Z, Song T, Wei C, Ma H, Ma Q, Zhang Y, Xu Y, Shi W, Ye Q, Zhong H, c-Abl regulates estrogen receptor alpha transcription activity through its stabilization by phosphorylation, *Oncogene* 29(15) (2010) 2238–2251. [PubMed: 20101225]
- [70]. Weigelt B, Lo AT, Park CC, Gray JW, Bissell MJ, HER2 signaling pathway activation and response of breast cancer cells to HER2-targeting agents is dependent strongly on the 3D microenvironment, *Breast Cancer Res. Treat* 122(1) (2010) 35–43. [PubMed: 19701706]
- [71]. Jung YS, Lee SJ, Yoon MH, Ha NC, Park BJ, Estrogen receptor  $\alpha$  is a novel target of the Von Hippel-Lindau protein and is responsible for the proliferation of VHL-deficient cells under hypoxic conditions, *Cell Cycle* 11(23) (2012) 4462–4473. [PubMed: 23159849]
- [72]. Connolly E, Braunstein S, Formenti S, Schneider RJ, Hypoxia inhibits protein synthesis through 4E-BP1 and elongation factor 2 kinase pathway controlled by mTOR and uncoupled in breast cancer cells, *Mol. Cell Biol* 26(10) (2006) 3955–3965. [PubMed: 16648488]
- [73]. Klinge CM, Estrogen receptor interaction with co-activators and co-repressors, *Steroids* 65(6) (2000) 2271–2251.
- [74]. Arany Z, Huang LE, Eckner R, Bhattacharya S, Jiang C, Goldberg MA, Bunn HF, Livingston DM, An essential role for p300/CBP in the cellular response to hypoxia, *Proc. Natl. Acad. Sci. USA* 93(23) (1996) 12969–12973. [PubMed: 8917528]
- [75]. Zhao W, Chang C, Cui Y, Zhao X, Yang J, Shen L, Zhou J, Hou Z, Zhang Z, Ye C, Hasenmayer D, Perkins R, Huang X, Yao X, Yu L, Huang R, Zhang D, Guo H, Yan J, Steroid receptor coactivator-3 regulates glucose metabolism in bladder cancer cells through coactivation of hypoxia inducible factor 1 $\alpha$ , *J. Biol. Chem* 289(16) (2014) 11219–11229. [PubMed: 24584933]
- [76]. Sotoca AM, van den Berg H, Vervoort J, van der Saag P, Strom A, Gustafsson JA, Rietjens I, Murk AJ, Influence of cellular ERalpha/ERbeta ratio on the ERalpha-agonist induced proliferation of human T47D breast cancer cells, *Toxicol. Sci* 105(2) (2008) 303–311. [PubMed: 18644836]

**Highlights:**

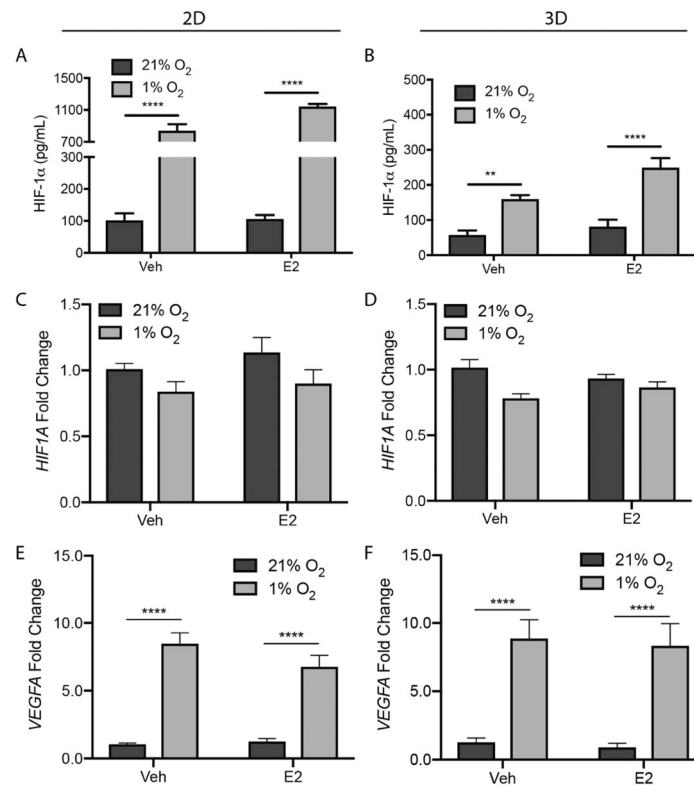
- ER $\alpha$  levels in 3D cultures are insensitive to hypoxia.
- Hypoxia decreases ER $\alpha$  transcriptional activity in 2D and 3D culture formats.
- HIF-1 $\alpha$  mediates the observed hypoxic responses in both culture formats.

**Fig. 1.**

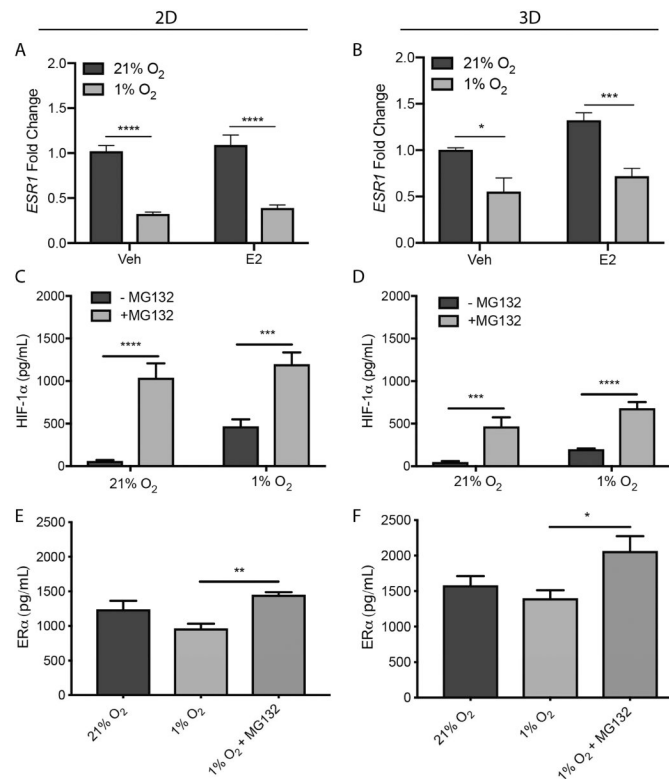
(A) Schematics of the 2D and 3D culture formats used throughout this work. Both formats contained 40,000 T47D cells that were either plated directly in a commercial 96 well plate or suspended in collagen I and seeded into a paper-based scaffold with a  $1 \times 10^{-3} \text{ cm}^3$  culture zone. Once seeded, the paper-based scaffolds were also placed in a commercial 96 well plate. All experiments were incubated under normoxic (21% O<sub>2</sub>) or hypoxic (1% O<sub>2</sub>) conditions in E2-deprived (Veh) or -supplemented (E2) medium for 24 h. (B, C) Average  $\pm$  SEM of ER $\alpha$  protein levels for each experimental condition determined by ELISA. Protein levels were normalized to  $\beta$ -actin. Each bar represents  $n = 12$  replicate cultures from three different cell passages. \* $p < 0.05$ , \*\* $p < 0.01$ , \*\*\* $p < 0.001$ , \*\*\*\* $p < 0.0001$ . (D) A representative western blot of ER $\alpha$  protein levels with a  $\beta$ -actin loading control.



**Fig. 2.** Representative single-plane confocal fluorescence micrographs of T47D cells in (A) 2D and (B) 3D culture formats after a 24 h incubation under normoxic (21% O<sub>2</sub>) or hypoxic (1% O<sub>2</sub>) conditions in E2-deprived (Veh) or -supplemented (E2) medium. Cells were fixed, immunostained for ERα (red), and the nuclei co-stained with DAPI (blue). The scale bar in each image represents 50 μm. Nuclear ERα values were normalized to the normoxic vehicle control for the 2D and 3D cultures. Frequency distributions of ERα staining, plotted for both (C) 2D and (D) 3D culture formats. ERα staining intensity, plotted as average ± SEM for both (E) 2D and (F) 3D culture formats. Each data is n > 150 nuclei from four replicate cultures from a total of two passages of cells. \**p* 0.05, \*\**p* 0.01, \*\*\**p* 0.001, \*\*\*\**p* 0.0001.

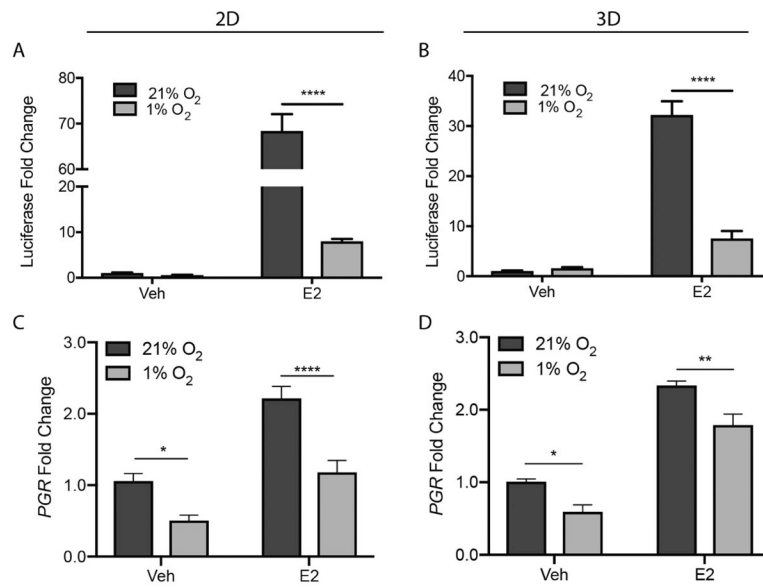


**Fig. 3.** 2D and 3D T47D cultures under normoxic (21% O<sub>2</sub>) or hypoxic (1% O<sub>2</sub>) conditions in E2-depleted (Veh) or E2-supplemented (E2) medium for 24 h, and then probed with ELISA to quantify HIF-1α protein levels (A, B). Protein levels were normalized to β-actin. Data represent the average ± SEM, from n = 12 replicate cultures from three different cell passages. Total RNA was extracted, and the relative expression of *HIF1A* (C, D) and *VEGFA* (E, F) for each experimental condition determined using the C<sub>t</sub> method; β-actin served as the reference gene. Data represent the average ± SEM, from n = 9 replicate cultures from a total of three passages of cells. \*p < 0.05, \*\*p < 0.01, \*\*\*p < 0.001, \*\*\*\*p < 0.0001.

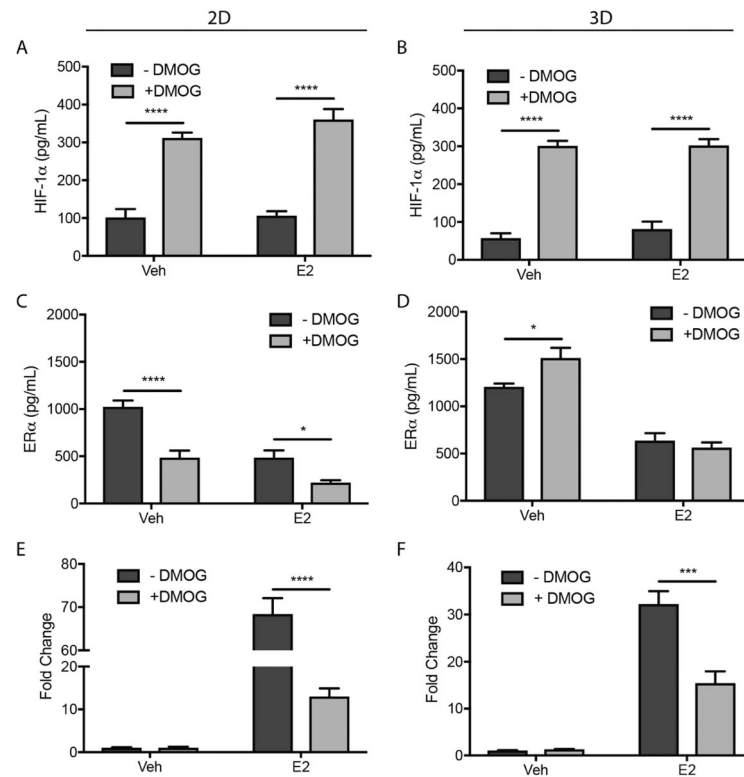
**Fig. 4.**

2D and 3D T47D cultures exposed to normoxic or hypoxic conditions in E2-deprived (Veh) or -supplemented (E2) medium for 24 h. Total RNA was extracted and relative expression of *ESR1* (A, B) was determined using the  $C_t$  method;  $\beta$ -actin served as the reference gene. Data represent the average  $\pm$  SEM, from  $n = 9$  replicate cultures from three different cell passages. 2D and 3D T47D cultures were exposed to normoxic or hypoxic conditions in estrogen-deprived medium in the presence or absence of MG-132 (10  $\mu$ M) for 8 h. HIF-1 $\alpha$  (C, D) and ER $\alpha$  (E, F) protein levels were quantified with ELISA. Data represent the average  $\pm$  SEM, from  $n = 6$  replicate cultures from two different cell passages. \* $p < 0.05$ , \*\* $p < 0.01$ , \*\*\* $p < 0.001$ , \*\*\*\* $p < 0.0001$ .



**Fig. 5.**

ER $\alpha$  transcriptional activation is reduced under hypoxic conditions in both 2D and 3D culture formats. Both culture formats were incubated in E2-deprived (Veh) or -supplemented (E2) medium under normoxic or hypoxic conditions for 24 h. Luciferase activity was quantified using the ONE-Glo luciferase assay; the fold-change in luminescence relative to E2-deprived cultures under normoxia was plotted for 2D (A) and 3D (B) culture formats. Figures represent the average  $\pm$  SEM, from  $n = 6$  replicates from three different cell passages. Total RNA was extracted and the relative expression of *PGR* mRNA (C, D) was determined using the  $C_t$  method;  $\beta$ -actin served as the reference gene. Data represent the average  $\pm$  SEM, from  $n = 9$  replicate cultures from three different cell passages \* $p < 0.05$ , \*\* $p < 0.01$ , \*\*\* $p < 0.001$ , \*\*\*\* $p < 0.0001$ .

**Fig. 6.**

T47D cells in 2D and 3D culture formats were incubated in the absence or presence of 1 mM DMOG for 1 h before culture in E2-deprived (Veh) or -supplemented (E2) medium ( $\pm$  DMOG) for 24 h. ELISA was used to quantify HIF-1 $\alpha$  (A, B) and ER $\alpha$  (C, D) protein levels which were normalized to  $\beta$ -actin. ER $\alpha$  transcriptional activity was measured using the ONE-Glo luciferase activity assay (E, F). Data represent the average  $\pm$  SEM from  $n = 6$  replicate cultures from at least two different cell passages.